

RESEARCH ARTICLE

Physically Realizable Antenna Equivalent Circuit Generation

MICAH P. HAACK¹, (Student Member, IEEE), RONALD P. JENKINS¹, (Member, IEEE), WENDING MAI¹, (Senior Member, IEEE), GALESTAN MACKERTICH-SENGERDY¹, (Member, IEEE), SAWYER D. CAMPBELL¹, (Senior Member, IEEE), MARIO F. PANTOJA², (Senior Member, IEEE), AND DOUGLAS H. WERNER¹, (Fellow, IEEE)

¹Department of Electrical Engineering, The Pennsylvania State University, University Park, PA 16802, USA

²Department of Electromagnetics and Physics Matter, University of Granada, 18071 Granada, Spain

Corresponding author: Micah P. Haack (mph6090@psu.edu)

This work was supported in part by the Salvador de Madariaga Program under Grant PRX21/00745, and in part by an endowment from the Penn State University McCain Chair Professorship.

ABSTRACT

This work introduces a new equivalent circuit generation method which can compute an accurate equivalent circuit representation for the known/measured impedance characteristics of antennas, which may assist in matching circuit design, non-Foster matching network design, and deep-learning antenna design. The method utilizes a modified Drude-Lorentz resonator representation inspired by optical material dispersion modeling to create multiple sub-circuits based on determined resonances in the impedance spectrum. Each computed sub-circuit is necessarily composed of physically realizable resistors, capacitors, and inductors, and they are connected in series to accurately reconstruct the device's corresponding impedance characteristics over a specified region of interest. The process is automated and applicable to a wide range of antennas and electromagnetic devices with multiple resonance phenomena. Current equivalent circuit design methods are limited by a lack of generalization and can require complex, active, or non-realizable circuit topologies. The proposed Drude-Lorentz-based approach can provide valuable insight into an antenna's resonant behavior while remaining general-purpose and only requiring passive components which are physically realizable. This improved generality is achieved by not requiring physical insights, but rather only utilizing the impedance data alone. Additionally, the method creates simpler circuits than other general methods, requiring less components and component types. This method is employed to create equivalent circuits of four different exemplary types of antennas, a patch antenna, a loop antenna, a spherical helix antenna, and a metantenna unit cell. The impedances generated from these circuit examples are compared with results of their full-wave simulation counterparts and found to be in excellent agreement.

INDEX TERMS Antenna equivalent circuit, Drude-Lorentz model, physically realizable circuit.

I. INTRODUCTION

Equivalent circuits of antennas are useful for a range of design needs, including miniaturization [1], determining broadband matching potential [2], and estimating antenna array performance [3]. Methods for creating equivalent circuits of antennas are varied. Techniques such as terminal eigenadmit-

The associate editor coordinating the review of this manuscript and approving it for publication was Ravi Kumar Gangwar¹.

tance, orthogonal spherical wave analysis, and Schelkunoff or Kings-Middleton approximations can be employed to create equivalent circuits of dipole antennas [4]. When creating patch antenna equivalent circuits, some approaches include the genetic algorithm or other optimization techniques [5], mode expansions [2], or relating the circuit components to the physical properties of the patch antenna [6]. In such cases, unit cell equivalent circuits require complex configurations and transformers [7].

Due to the focus on the properties of specific designs, existing equivalent circuit methods have difficulty being applied to a broader class of antennas. While more general methods to fit multiple types of antennas exist, they are limited as they typically require a significant number of circuit components or terms to fit a single resonance [8], or necessitate the imposition of difficult constraints to ensure a physically realizable circuit [9]. Additionally, general methods often require more component types than resistors, capacitors, and inductors.

Due to the Drude-Lorentz model's effectiveness at representing highly dispersive systems with multiple resonances, it has seen success in optical applications for material permittivity approximation [10], [11]. Drude-Lorentz models have also been shown to be extendable to circuit forms for atomic models, but these approaches have required non-passive components such as voltage sources, as well as non-physical components in the form of a half-capacitor [12].

This paper improves upon the limitations described for existing equivalent circuit generation methods by providing a generalized and simpler circuit model that requires only a single circuit term per resonance in the impedance data. The method presented also improves existing Drude-Lorentz circuit models by implementing the equivalent circuit using only physically realizable and passive components. We define a physically realizable equivalent circuit as one that can be achieved with only passive components (for this method, only resistors, capacitors, and inductors) that do not require negative values, and as such can be created with commercial off-the-shelf (COTS) parts. Importantly, to ensure a physically realizable circuit the method introduces a single linear constraint that is simpler to enforce than the constraints from other reported equivalent circuit generation methods.

The Drude-Lorentz based approach provides several benefits over existing equivalent circuit models. The simple structure of the equivalent circuit model presented in this work can be easily inverted to create non-Foster matching network designs [13]. The equation link presented between the Drude-Lorentz parameters and impedance provides a connection between full-wave electromagnetic solvers and high-performance circuit simulation programs that can be difficult to achieve otherwise. Additionally, the increase in the application of deep-learning approaches in antenna design is a rapidly developing field. Consequently, methods to quickly create equivalent circuits can be directly employed as surrogate models for dataset generation or they can even be directly used in deep-learning methods to produce optimized designs [14]. While construction of antenna equivalent circuits is a robust research area, the specific benefits of speed, generality, and simplicity of the Drude-Lorentz method presented here is expected to be particularly beneficial in non-Foster matching, and deep-learning design approaches.

This paper introduces a new methodology based on a Drude-Lorentz model extended from optical [11] to RF frequencies to create simple equivalent circuit models for multiple antennas, with only a single circuit term required for each resonance of interest. To achieve this, Section II

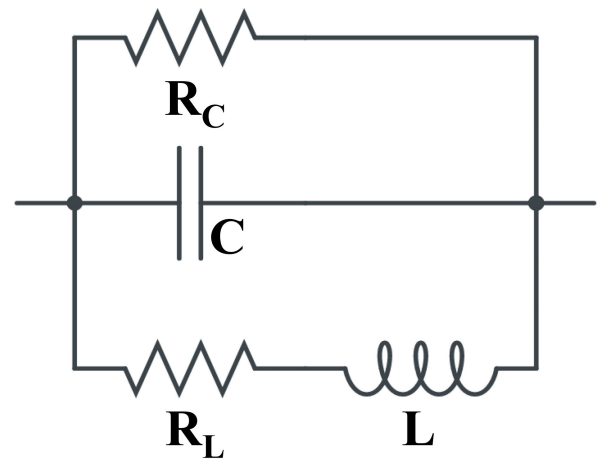


FIGURE 1. Circuit applied for each term in the Drude-Lorentz model summation. Additional terms are connected in series.

introduces a Drude-Lorentz kernel and the corresponding impedance expression for an equivalent circuit term. Then the two expressions are equated, resulting in a set of equations which are solved to find the circuit component values in terms of the Drude-Lorentz model parameters. Next, the required constraints to ensure physically realizable circuits are introduced. The equivalent circuit generation method is applied to four different antennas (a patch antenna, a loop antenna, a metantenna unit cell [15], and a spherical helix antenna) to generate their equivalent circuits for a targeted region of interest, and the results are compared to full-wave simulated data obtained from Ansys HFSS [16].

II. METHOD

A. DRUDE-LORENTZ MODEL

The conversion process begins with a modified Drude-Lorentz model defined in (1), where the σ term is assumed to be purely real valued. This model is an extension of the previous optical Drude-Lorentz model provided by [11]. The modification to the real-valued σ term enables the circuit conversion process by allowing the same mathematical form as the circuit impedance expression. The number of Drude-Lorentz terms used corresponds to the number of desired resonances to create, and F represents the feature of interest, such as permittivity or impedance. When creating the circuits, the designer can specify how many resonant terms (and thus how many resonant circuit terms) by selecting the region of interest for the impedance data. This flexibility allows for any number of desired resonant terms. In this case F refers to the impedance of the desired antenna resonance. Fitting the antenna impedance data obtained from Ansys HFSS [16] to the Drude-Lorentz model is accomplished with a curve-fitting process implemented in Python. This approach is carried out with a least-squares technique applied over the targeted operating region, with the number of Drude-Lorentz terms equal to the number of resonances desired to fit. For the derivation presented here, only a single circuit

term and impedance resonance is analyzed, as the procedure is identical for every circuit term that is added in series. Extending the circuit to more resonances is accomplished by summing additional Drude-Lorentz resonators and adding the corresponding circuit terms in series with the others. We define $\omega = 2\pi f$, where f is the frequency. The variables Ω_R , Ω_I , and σ_R are the fitting variables that are based on the model from [11]. Equations (2) through (6) follow the derivation to convert the Drude-Lorentz model into a single fraction, in which the coefficients A_1 through A_4 are the terms that will be used to equate to the circuit model in Fig. 1. The j^2 values are left un-simplified to clearly show the Drude-Lorentz form and the impedance form are identical and as such can be related.

$$F = (-j\sigma_R) \left[\frac{1}{\omega - \Omega} + \frac{1}{\omega + \Omega^*} \right] \quad (1)$$

$$F = (-j\sigma_R) \left[\frac{\omega + \Omega_R - j\Omega_I + \omega - \Omega_R - j\Omega_I}{(\omega - \Omega_R - j\Omega_I)(\omega + \Omega_R - j\Omega_I)} \right] \quad (2)$$

$$F = (-j\sigma_R) \left[\frac{2\omega - j2\Omega_I}{\omega^2 - j\omega 2\Omega_I - \Omega_R^2 - \Omega_I^2} \right] \quad (3)$$

$$F = (j\sigma_R) \left[\frac{2\omega - j2\Omega_I}{j^2\omega^2 + j\omega 2\Omega_I + \Omega_R^2 + \Omega_I^2} \right] \quad (4)$$

$$F = \frac{j\omega 2\sigma_R + 2\sigma_R\Omega_I}{j^2\omega^2 + j\omega 2\Omega_I + \Omega_R^2 + \Omega_I^2} \quad (5)$$

$$F = \frac{j\omega A_1 + A_2}{j^2\omega^2 + j\omega A_3 + A_4} \quad (6)$$

$$A_1 = 2\sigma_R \quad A_2 = 2\sigma_R\Omega_I \quad A_3 = 2\Omega_I \quad A_4 = \Omega_R^2 + \Omega_I^2 \quad (7)$$

B. EQUIVALENT CIRCUIT IMPEDANCE

The equivalent circuit from Fig. 1 will be used to equate the impedance and Drude-Lorentz model from (1). This circuit topology was chosen since the RLC structure provides a mathematically convenient resonator representation for the impedance to equate to the form of the Drude-Lorentz model in (6). The impedance in (8) needs to be re-arranged to match the same form as (6). To achieve this, we start by introducing the circuit impedance in (8) as:

$$\frac{1}{Z} = \frac{1}{R_C} + j\omega C + \frac{1}{R_L + j\omega L} \quad (8)$$

where R_C , C , R_L , and L are the circuit components defined in Fig. 1. The impedance in (8) is rearranged in (9) through (11) to match the form from the modified Drude-Lorentz model:

$$\frac{1}{Z} = \frac{1 + j\omega R_C C}{R_C} + \frac{1}{R_L + j\omega L} \quad (9)$$

$$\frac{1}{Z} = \frac{j^2\omega^2 L R_C C + j\omega(L + R_L R_C C) + R_C + R_L}{j\omega R_C L + R_C R_L} \quad (10)$$

Dividing by $L R_C C$ and rearranging, a matching expression for the Drude-Lorentz model from (6) is found using circuit components. The B coefficients introduced in (12) will be

equated to the A coefficients from (7) to solve for the circuit component values.

$$Z = \frac{j\omega B_1 + B_2}{j^2\omega^2 + j\omega B_3 + B_4} \quad (11)$$

$$B_1 = \frac{1}{C} \quad B_2 = \frac{R_L}{LC} \quad B_3 = \frac{L + R_L R_C C}{L R_C C} \quad B_4 = \frac{R_C + R_L}{L R_C C} \quad (12)$$

C. OBTAINING CIRCUIT PARAMETERS

Since (6) and (11) are the same form, finding the circuit values from the Drude-Lorentz parameters is accomplished by equating the A coefficients from (7) with the B coefficients from (12) and solving for the component values. First, we express the corresponding combined equations as:

$$\frac{1}{C} = 2\sigma_R \quad (13)$$

$$\frac{R_L}{CL} = 2\sigma_R\Omega_I \quad (14)$$

$$\frac{R_L R_C C + L}{CL R_C} = 2\Omega_I \quad (15)$$

$$\frac{R_C + R_L}{CR_C L} = \Omega_R^2 + \Omega_I^2 \quad (16)$$

The first component C can be directly solved for.

$$C = \frac{1}{2\sigma_R} \quad (17)$$

By combining (15), (16), and (17), R_C can be found.

$$\frac{R_L}{L} + \frac{1}{CR_C} = 2\Omega_I \quad (18)$$

$$R_C = \frac{2\sigma_R}{\Omega_I} \quad (19)$$

Next, L can be obtained with (14), (16), (17), and (19).

$$\frac{2\sigma_R}{L} + \frac{2\sigma_R\Omega_I}{R_C} = \Omega_R^2 + \Omega_I^2 \quad (20)$$

$$L = \frac{2\sigma_R}{\Omega_R^2} \quad (21)$$

Finally, R_L is solved for with (14), (17), and (21).

$$R_L = \frac{2\sigma_R\Omega_I}{\Omega_R^2} \quad (22)$$

To verify that the equivalent circuit impedance was identical to (11), the circuit components from (17), (19), (21), and (22) were simulated in the circuits from Fig. 1 using PathWave Advanced Design System (ADS) [17], and the impedance curve validated with the expected Drude-Lorentz impedance data. For all antenna examples presented, the resulting equivalent circuits were also simulated and validated using ADS, and compared with the antenna impedance data.

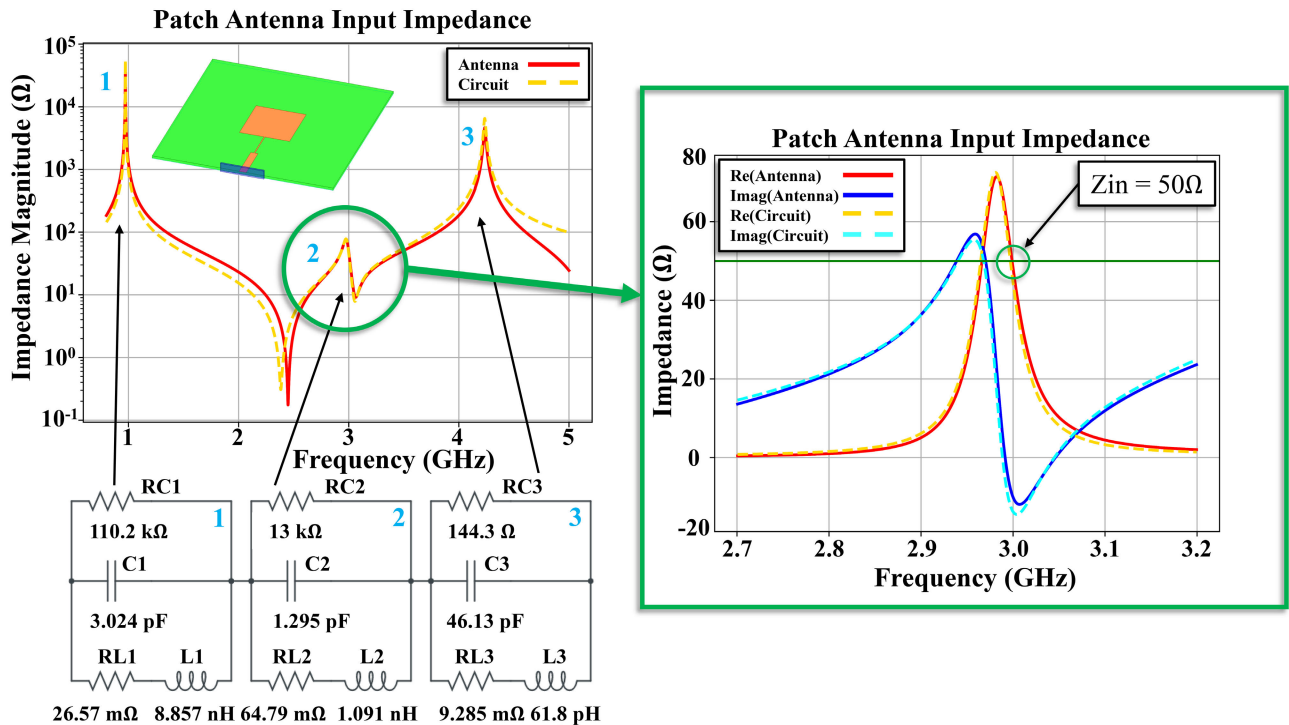


FIGURE 2. Patch antenna designed for 3 GHz and associated equivalent circuit result. Three resonances are shown in a magnitude log plot and a zoomed in area of the operating range is provided in real and imaginary components. Each circuit section creates one resonance in the impedance equivalent, corresponding from left to right and indicated with arrows. The zoomed in area of the operating region shows a real 50 Ω match at the 3 GHz operating frequency and is indicated with a horizontal green line.

D. ENSURING POSITIVE COMPONENT VALUES

In order to generate a circuit with positive resistor values (and ensure the circuit components are physically realizable) boundaries on the model variables need to be enforced. The necessary restriction can be found by examining the circuit component expressions from (17), (19), (21), and (22). Since Ω_1 corresponds to the resonance locations on the frequency axis, the value will always be positive, and can be ignored. Ω_R^2 in the denominator of (21) and (23) will also always be a positive quantity, so the only possible value that could cause a component to assume a negative value is σ_R . As such, the only boundary that needs to be enforced to ensure positive component values is:

$$\sigma_R > 0 \tag{23}$$

This is a linear constraint and can easily be applied to most curve fitting or optimization routines.

III. RESULTS

A. PATCH ANTENNA EXAMPLE

To provide an example of using the process introduced in Section II, a patch antenna equivalent circuit is created and shown in Fig. 2. The patch antenna is designed to operate at 3 GHz and is simulated in Ansys HFSS [16]. The dimensions of the patch are 27.6 mm wide by 27.6 mm long, and the S_{11} of the patch is -19.61 dB at 3 GHz. The equivalent circuit method is applied to the antenna impedance data and is

displayed in a semilog plot of the magnitude. Each resonance location is represented by an individual circuit term which is numbered. While the fit was done over the operating region (2.7 GHz to 3.2 GHz), three circuit terms were used in the complete impedance data. The operating region is shown in real and imaginary impedance components and matches well with the antenna data over the region of interest. The zoomed in section shows the 50 Ω crossing on the real impedance, where the patch antenna is well matched. Due to smaller errors near this location having a large impact on the performance of the antenna equivalent circuit, some accuracy on the out of band resonances was traded for increased accuracy at the operating region.

B. OTHER ANTENNA EXAMPLES

The circuit generation method is additionally applied to three other antenna examples to emphasize the generality of the method and are shown in Fig. 3. These are a loop antenna, a metantenna unit cell [15], and a spherical helix antenna. All antenna examples were modeled using Ansys HFSS [16]. The loop antenna has a 3.63 cm diameter and 1.16 mm wire diameter with a S_{11} of -17.1 dB at 3 GHz. The metantenna unit cell example is shown to further emphasize the generality of the method, as it is a unique example merging metamaterials, array unit cells, and artificial magnetic conducting (AMC) surfaces. However, the metantenna unit cell itself is a primary resonator and can be considered as an antenna

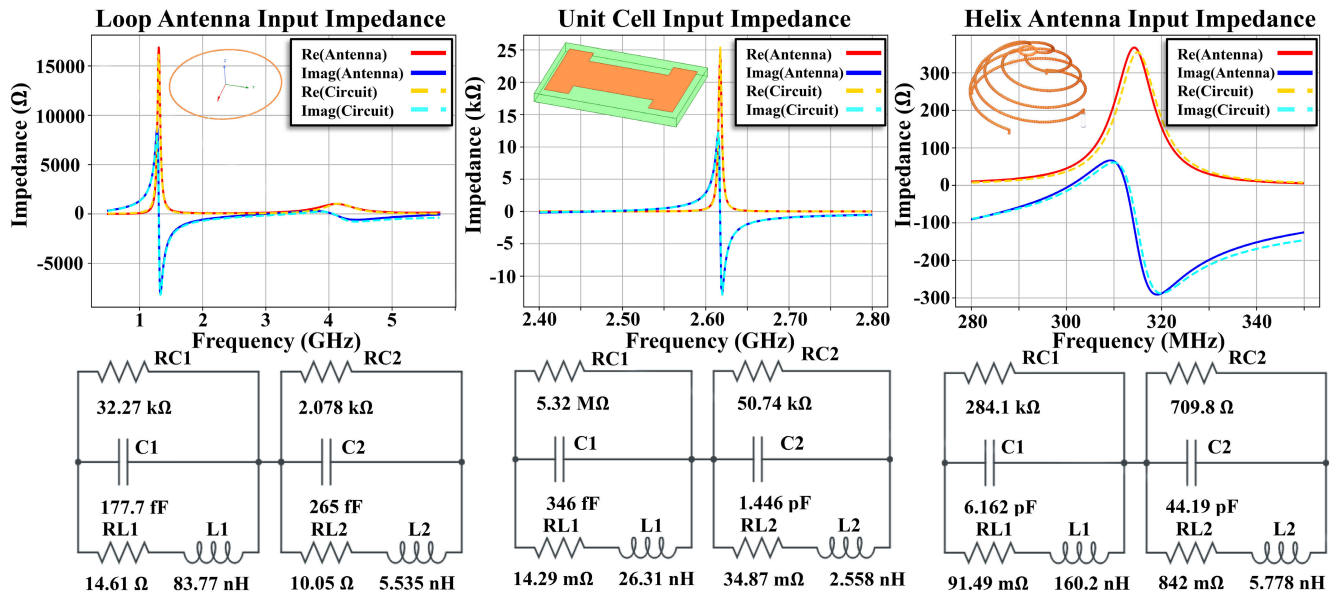


FIGURE 3. Three antenna equivalent circuit model examples are shown in order, a loop antenna, a metantenna unit cell, and a spherical helix antenna. The loop antenna contained both resonances in its operating region of $f = 1$ GHz to $f = 5$ GHz. The metantenna operating region was fit over $f = 2.4$ GHz to $f = 2.8$ GHz with an out of band resonance located at $f = 1.67$ GHz at an impedance value of $Z = 166 \text{ k}\Omega + j840 \text{ k}\Omega$. The spherical helix operating region was fit over $f = 280$ MHz to $f = 340$ MHz, with an out of band resonance located at $f = 160$ MHz at an impedance value of $Z = 120 \text{ k}\Omega + j82.2 \text{ k}\Omega$. The Ansys HFSS models of the antennas are included as an inset in each plot.

for the example’s purposes [15]. The metantenna unit cell dimensions are too complex to include here but can be found in [15]. The spherical helix is a four-arm design (single-monopole feed and remaining arms shorted to ground) with a height of 58.9 mm, a wire diameter of 2.6 mm, a top ring radius of 8.5 mm, and a bottom diameter of 117.8 mm. The spherical helix antenna has a S_{11} of -36.7 dB at 300 MHz.

Since the metantenna unit cell and spherical helix antenna have very large resonances outside the operating frequency in the impedance regime, only the operating frequencies of interest are shown in Fig. 3 to increase the readability of the plots. The linear constraint from (23) was applied to all examples and did not cause additional difficulty when generating the equivalent circuit models, resulting in entirely passive physically realizable components and no negative values.

IV. CHALLENGES

When creating equivalent circuits with a Drude-Lorentz approach, some challenges can arise during fitting procedures. A significant one can be found when fitting antennas using multiple closely spaced resonances or overlapping ones. These challenges are complicated to resolve, and since the primary focus of this method is the connection between the Drude-Lorentz form and the impedance representations, overcoming these is not covered in depth. However, methods exist in literature for overcoming the challenges of overlapping resonances, and a recommended starting point can be found in [18]. Additionally, a second challenge in applying the method can be found when matching the impedance

at low frequencies (e.g., the capacitive impedance behavior observed for dipole antennas at asymptotically low frequencies). This can be overcome by adding a simpler circuit term containing only a capacitor outside of the normal Drude-Lorentz terms.

V. CONCLUSION

This paper introduced an equivalent circuit generation method based on Drude-Lorentz resonators. Limitations of existing equivalent circuit models for antennas include difficulty in applying them to any general type instead of specific ones and requiring circuit components aside from resistors, capacitors, and inductors, or even components that are not physically realizable. Our method improves on the generalization limitation of other methods and is validated by creating equivalent circuit models for a variety of different antenna examples, including a patch antenna, a loop antenna, a metantenna unit cell for a larger transmit array, and a spherical helix antenna. The proposed method also improves on existing limitations of equivalent circuit models which rely on non-physically realizable circuit components by requiring only a single, easy to enforce linear constraint that ensures all components will be passive and physically realizable. Previous general methods, especially the method in [9], require complex circuits with transformers, while the Drude-Lorentz method described only utilizes resistors, capacitors, and inductors combined in a simpler configuration. Each circuit term in the Drude-Lorentz method corresponds directly to an observed resonance in the impedance spectrum. The method is not intended to model the antenna’s behavior from DC to

arbitrarily high frequencies, but rather produces an equivalent circuit for the antenna over a user defined frequency region of interest. The equivalent circuits generated from the method presented in this work can be used in place of difficult and time consuming full-wave simulations. Important applications include its use in tasks such as antenna impedance matching or full system analysis by employing simpler and faster circuit simulators for expensive optimization studies. Additionally, ongoing research areas in non-Foster matching network design [13] and deep-learning accelerated antenna design [14] can exploit the benefits of the equivalent circuit method presented herein.

REFERENCES

- [1] Y.-S. Wang and S.-J. Chung, "A short open-end slot antenna with equivalent circuit analysis," *IEEE Trans. Antennas Propag.*, vol. 58, no. 5, pp. 1771–1775, May 2010, doi: [10.1109/TAP.2010.2044471](https://doi.org/10.1109/TAP.2010.2044471).
- [2] M. Ansari-zadeh, A. Ghorbani, and R. A. Abd-Alhameed, "An approach to equivalent circuit modeling of rectangular microstrip antennas," *Prog. Electromagn. Res. B*, vol. 8, pp. 77–86, 2008, doi: [10.2528/pierb08050403](https://doi.org/10.2528/pierb08050403).
- [3] B. Wang, X. Q. Lin, L. Y. Nie, and D. Q. Yu, "A broadband wide-scanning planar phased array antenna with equivalent circuit analysis," *IEEE Antennas Wireless Propag. Lett.*, vol. 19, pp. 2154–2158, 2020, doi: [10.1109/LAWP.2020.3025340](https://doi.org/10.1109/LAWP.2020.3025340).
- [4] T. G. Tang, Q. M. Tieng, and M. W. Gunn, "Equivalent circuit of a dipole antenna using frequency-independent lumped elements," *IEEE Trans. Antennas Propag.*, vol. 41, no. 1, pp. 100–103, Jan. 1993, doi: [10.1109/8.210122](https://doi.org/10.1109/8.210122).
- [5] P. L. Werner, R. Mittra, and D. H. Werner, "Extraction of equivalent circuits for microstrip components and discontinuities using the genetic algorithm," *IEEE Microw. Guided Wave Lett.*, vol. 8, no. 10, pp. 333–335, Oct. 1998, doi: [10.1109/75.735412](https://doi.org/10.1109/75.735412).
- [6] F. Abboud, J. P. Damiano, and A. Papiernik, "Simple model for the input impedance of coax-fed rectangular microstrip patch antenna for CAD," *IEE Proc. H Microw., Antennas Propag.*, vol. 135, no. 5, pp. 323–326, Oct. 1988, doi: [10.1049/ip-h-2.1988.0066](https://doi.org/10.1049/ip-h-2.1988.0066).
- [7] G. Perez-Palomino and J. E. Page, "Bimode Foster's equivalent circuit of arbitrary planar periodic structures and its application to design polarization controller devices," *IEEE Trans. Antennas Propag.*, vol. 68, no. 7, pp. 5308–5321, Jul. 2020, doi: [10.1109/TAP.2020.2976506](https://doi.org/10.1109/TAP.2020.2976506).
- [8] Y. Wang, J. Li, and L.-X. Ran, "An equivalent circuit modeling method for ultra-wideband antennas," *Prog. Electromagn. Res.*, vol. 82, pp. 433–445, 2008, doi: [10.2528/pier08032303](https://doi.org/10.2528/pier08032303).
- [9] Y. Kim and H. Ling, "Equivalent circuit modeling of broadband antennas using a rational function approximation," *Microw. Opt. Technol. Lett.*, vol. 48, no. 5, pp. 950–953, May 2006, doi: [10.1002/mop.21529](https://doi.org/10.1002/mop.21529).
- [10] E. Silaeva, L. Saddinger, and J.-P. Colombier, "Drude-Lorentz model for optical properties of photoexcited transition metals under electron-phonon nonequilibrium," *Appl. Sci.*, vol. 11, no. 21, p. 9902, Oct. 2021, doi: [10.3390/app11219902](https://doi.org/10.3390/app11219902).
- [11] H. S. Sehmi, W. Langbein, and E. A. Muljarov, "Optimizing the Drude-Lorentz model for material permittivity: Method, program, and examples for gold, silver, and copper," *Phys. Rev. B, Condens. Matter*, vol. 95, no. 11, Mar. 2017, Art. no. 115444, doi: [10.1103/physrevb.95.115444](https://doi.org/10.1103/physrevb.95.115444).
- [12] C. A. Gonano and R. E. Zich, "Drude-Lorentz model in circuit form," in *Proc. 8th Eur. Conf. Antennas Propag. (EuCAP)*, Apr. 2014, pp. 1518–1521, doi: [10.1109/EuCAP.2014.6902071](https://doi.org/10.1109/EuCAP.2014.6902071).
- [13] S. E. Sussman-Fort, "Matching network design using non-Foster impedances," *Int. J. RF Microw. Comput.-Aided Eng.*, vol. 16, no. 2, pp. 135–142, 2006, doi: [10.1002/mmce.20118](https://doi.org/10.1002/mmce.20118).
- [14] Z. Wei, Z. Zhou, P. Wang, J. Ren, Y. Yin, G. F. Pedersen, and M. Shen, "Equivalent circuit theory-assisted deep learning for accelerated generative design of metasurfaces," *IEEE Trans. Antennas Propag.*, vol. 70, no. 7, pp. 5120–5129, Jul. 2022, doi: [10.1109/TAP.2022.3152592](https://doi.org/10.1109/TAP.2022.3152592).
- [15] Z. H. Jiang, D. E. Brocker, P. E. Sieber, and D. H. Werner, "A compact, low-profile metasurface-enabled antenna for wearable medical body-area network devices," *IEEE Trans. Antennas Propag.*, vol. 62, no. 8, pp. 4021–4030, Aug. 2014, doi: [10.1109/TAP.2014.2327650](https://doi.org/10.1109/TAP.2014.2327650).
- [16] *Ansys Electronics Desktop Version 2021.6.2*, Ansys, Canonsburg, PA, USA, 2021.
- [17] *PathWave Advanced Design System (ADS) 2021 Update 2*, Keysight, Santa Rosa, CA, USA, 2021.
- [18] D. T. Stibbe and J. Tennyson, "TIMEDEL: A program for the detection and parameterization of resonances using the time-delay matrix," *Comput. Phys. Commun.*, vol. 114, nos. 1–3, pp. 236–242, Nov. 1998, doi: [10.1016/s0010-4655\(98\)00070-8](https://doi.org/10.1016/s0010-4655(98)00070-8).



MICAH P. HAACK (Student Member, IEEE) was born in Butte, Montana, in 1998. He received the B.S. degree in electrical engineering from Grove City College, PA, USA, in 2021, with a focus on computer engineering. He is currently pursuing the Ph.D. degree in electrical engineering with the Computational Electromagnetics and Antennas Research Laboratory (CEARL), The Pennsylvania State University, with a focus on antenna design, under the guidance of Prof. Werner.

He is a member of the American Physical Society (APS).



RONALD P. JENKINS (Member, IEEE) received the B.S. degree in computer engineering from Grove City College, in 2016, and the Ph.D. degree in electrical engineering from The Pennsylvania State University, University Park, in 2022.

He is currently a Postdoctoral Scholar with the Computational Electromagnetics and Antennas Research Laboratory (CEARL), The Pennsylvania State University, under the supervision of Prof. Douglas Werner. His research interests include

computational electromagnetics, evolutionary algorithms, deep learning, multiobjective optimization, metasurfaces, optics, and nanophotonics.



WENDING MAI (Senior Member, IEEE) received the B.S. degree in electronic information science and technology, the M.S. degree in radio physics, and the Ph.D. degree in electromagnetic and microwave technology from the University of Electronic Science and Technology of China, Chengdu, China, in 2007, 2010, and 2019, respectively.

In 2009, he was a Student Researcher with the Lenovo Research Institute, Chengdu. Then, he became an Engineer with Texas Instrument, Shanghai and Dallas. From 2013 to 2015, he was an Assistant Professor with Xichang University. In 2017, he joined the Computational Electromagnetics and Antennas Research Laboratory, Department of Electrical Engineering, The Pennsylvania State University, as a Visiting Scholar, and then a Postdoctoral Scholar, under the supervision of Prof. Douglas H. Werner. Since 2022, he has been a Senior Research and Development Engineer with Ansys, Pittsburg, USA. He has published over 30 technical articles and proceeding articles. He served as a reviewer for over ten journals and NSF grants. His current research interests include computational electromagnetics (hp-adaptive technique, DGTD, and nonlinear and dispersive materials), knot, and time-varying electromagnetics.

Dr. Mai is a Life Member of OPTICA and ACES.



GALESTAN MACKERTICH-SENGERDY (Member, IEEE) received the B.S. degree in mechanical engineering and the M.S. degree in engineering science and mechanics from The Penn State University, University Park, PA, USA, where he is currently pursuing the Ph.D. degree in electrical engineering.

From 2009 to 2018, he worked in industry as a Senior Mechanical Engineer. Since 2019, he has been a Researcher with the Computational Electromagnetics and Antennas Research Laboratory, The Penn State University. He has expertise in designing mechanically robust, high-power, and metamaterial antenna systems. He is a member of the Directed Energy Professional Society and the Association of Old Crows.



SAWYER D. CAMPBELL (Senior Member, IEEE) received the B.S. degree in physics from Illinois Wesleyan University, Bloomington, IL, USA, in 2008, and the M.S. and Ph.D. degrees in optical sciences from The University of Arizona, Tucson, AZ, USA, in 2010 and 2013, respectively.

He was an Undergraduate Researcher with the Intense Laser Physics Theory Unit, Department of Physics, Illinois State University, from 2004 to 2008. He was a Graduate Research

Associate with the La Casa de Creative Electromagneticists, Department of Electrical and Computer Engineering, The University of Arizona, under the supervision of Prof. Richard W. Ziolkowski. In 2014, he joined the Computational Electromagnetics and Antennas Research Laboratory, Department of Electrical Engineering, The Pennsylvania State University, as a Postdoctoral Scholar, under the supervision of Prof. Douglas H. Werner. Since 2022, he has been an Associate Research Professor with the Department of Electrical Engineering, The Penn State University, and an Associate Director of the Computational Electromagnetics and Antennas Research Laboratory (CEARL). Additionally, he is an expert in the application of multi-objective and surrogate-assisted optimization techniques to challenging problems in both the RF and optical regimes. He has extensive experience in the computational modeling and inverse design of metamaterial- and transformation optics-based devices at RF, infrared, and optical frequencies. He has published over 180 technical articles and proceedings articles and two books. He is the author/coauthor of five book chapters. His current research interests include metasurfaces, nanophotonics, gradient-index lenses, high-power microwave antennas, optimization, and the applications of deep learning to RF and optical inverse-design problems.

Dr. Campbell is a Senior Member of OPTICA and SPIE. He is the past Chair and the current Vice-Chair/Treasurer of the IEEE Central Pennsylvania Section. Since 2023, he has been an Associate Editor of IEEE ACCESS.



MARIO F. PANTOJA (Senior Member, IEEE) received the B.S., M.S., and Ph.D. degrees in electrical engineering from the University of Granada, Granada, Spain, in 1996, 1998, and 2001, respectively.

Since 2016, he has been a Full Professor with the University of Granada. He has published more than 60 refereed journal articles and book chapters, and more than 100 conference papers and technical reports. He has participated in more than 50 national and international projects with public and private funding. He received grants to stay as a Visiting Scholar with Dipartimento Ingegneria dell'Informazione, University of Pisa, Italy; the International Research Centre for Telecommunications and Radar, Delft University of Technology, The Netherlands; and the Antenna and Electromagnetics Group, Denmark Technical University. In addition, he received the 2015 Fulbright Grant to collaborate with the Computational Electromagnetics and Antennas Research Laboratory, The Pennsylvania State University, USA. His research interests include the areas of time-domain analysis of electromagnetic radiation and scattering problems, optimization methods applied to antenna design, terahertz technology, bioelectromagnetics, and nanoelectromagnetics. He was a recipient of the 2002 International Union of Radio Science (URSI) Young Scientist Award.



DOUGLAS H. WERNER (Fellow, IEEE) received the B.S. and M.S. degrees in electrical engineering, the M.A. degree in mathematics, and the Ph.D. degree in electrical engineering from The Pennsylvania State University (Penn State), University Park, in 1983, 1985, 1986, and 1989, respectively.

He holds the John L. and Genevieve H. McCain Chair Professorship with the Department of Electrical Engineering, The Pennsylvania State University. He is currently the Director of the Computational Electromagnetics and Antennas Research Laboratory (CEARL: <http://cearl.ee.psu.edu/>), Penn State. He has published over 1000 technical articles and proceedings articles, 30 book chapters with several additional chapters currently in preparation, and eight books. His research interests include computational electromagnetics/optics (MoM, FEM, FEBI, FDTD, DGTD, CBFM, RCWA, GO, and GTD/UTD) and the development and application of multi-objective inverse-design techniques (topology optimization, genetic algorithms, clonal selection algorithms, particle swarm, wind-driven, ant colony, and various other evolutionary programming schemes). He has also made numerous key contributions in the areas of electromagnetic/optical wave interactions with complex media, metamaterials and metasurfaces, transformation optics, nanoscale electromagnetics (including nanoantennas), flat optics (including gradient index (GRIN) and metalenses), antenna theory and design (including wearable, e-textile, electrically small, GPS, 5G/6G, conformal, additively manufactured, and reconfigurable antennas), phased arrays (including ultra-wideband arrays), high-power microwave devices, wireless and personal communication systems (including on-body networks), frequency selective surfaces, and fractal and knot electrodynamics.

Dr. Werner is a fellow of eight professional societies, including IET, NAI, OPTICA, SPIE, ACES, AAIA, and the PIER Electromagnetics Academy. He is a Senior Member of the International Union of Radio Science (URSI).

•••